

Pavel Strnad · Reinhard Windoffer · Rudolf E. Leube

## In vivo detection of cytokeratin filament network breakdown in cells treated with the phosphatase inhibitor okadaic acid

Received: 25 May 2001 Accepted: 27 July 2001 / Published online: 25 September 2001  
© Springer-Verlag 2001

**Abstract** We have previously described vulva carcinoma-derived A-431 subclone AK13-1, which stably expresses fluorescently labeled cytokeratin filaments (CKFs). Time-lapse fluorescence microscopy of these cells permits the continuous monitoring of the dynamics of the CKF cytoskeleton in vivo. To study mechanisms and principles of CKF disassembly as it occurs, e.g., during mitosis and liver disease, we have treated cells with the phosphatase inhibitor okadaic acid (OA), which induces complete CKF network breakdown within 3–5 h without significantly affecting the organization of the actin- and tubulin-based cytofilaments. In time-lapse movies, we find that the network breakdown starts at the cell periphery and proceeds toward the cell center, where residual filaments become compacted into a prominent perinuclear ring. The progressing disassembly is paralleled by an increase of diffuse fluorescence throughout the cytoplasm and the appearance of non-filamentous spheroidal aggregates. They are formed in the filament-free cell periphery from non-filamentous precursors and can sometimes be detected in the proximity of desmosomes. Other aggregates are either found in close apposition to CKFs or are generated directly from the compacted perinuclear material. Primary granules later fuse, thereby producing structures of considerable size. We show that CKF network breakdown and granule formation rely on metabolic energy and that the continued presence of OA is needed for its completion. We conclude that phosphorylation/dephosphorylation is an important mechanism regulating CKF network dynamics in vivo with far-reaching implications for the understanding of epithelial plasticity and pathology.

**Keywords** Cytoskeleton · Intermediate filament · Phosphorylation · Green fluorescent protein · Time-lapse fluorescence microscopy · Cell culture · Human

### Introduction

The compositionally highly complex intermediate filaments (IFs), actin-based microfilaments, and tubulin-based microtubules define three major networks that are integrated with each other, thus forming the cytoskeleton of higher eukaryotic cells. On the basis of sequence similarities and assembly properties, six classes of IF polypeptides can be distinguished that are encoded by cell-type-specifically expressed multigene families (Fuchs and Weber 1994; Moll 1998). All polypeptides share the same basic molecular design (Fuchs and Weber 1994; Coulombe et al. 2000; Herrmann and Aebi 2000). The conserved central domain has an  $\alpha$ -helical conformation and interacts with partner IF polypeptides to generate coiled-coil structures. In contrast, the non-helical end domains vary considerably in length and amino acid composition. They are also the major targets for protein modification (Omary et al. 1998). The epithelial cytokeratin (CK) polypeptides, comprising more than 30 members, can be grouped into the smaller and more acidic type I CKs and the larger and more basic type II CKs (Fuchs and Weber 1994). They are obligatory heteropolymers, the type I and type II CKs associating in parallel and in register through the hydrophobic surface of their central  $\alpha$ -helical domains into very stable dimers that can only be disrupted with high concentrations of chaotropic agents (Coulombe and Fuchs 1990; Hatzfeld and Weber 1990; Steinert 1990). In general, specific pairs of type I and type II CKs are coexpressed, although alternative pairing occurs not only in vitro (Hatzfeld and Franke 1985; Hofmann and Franke 1997), but also in vivo (see Moll 1998 and references therein). Dimers associate in an antiparallel fashion to form non-polar tetramers that appear to be the major soluble CK form (Quinlan et al. 1984; Chou et al. 1993; Steinert and Marekov 1993; see,

This work was supported by grants from the “Stiftung Rheinland Pfalz für Innovation” and the German Research Council (LE 566/7). Movies are provided at <http://www.uni-mainz.de/FB/Medizin/Anatomie/Leube/>

P. Strnad · R. Windoffer · R.E. Leube (✉)  
Department of Anatomy, Johannes Gutenberg University Mainz,  
Becherweg 13, 55128 Mainz, Germany  
e-mail: leube@mail.uni-mainz.de  
Tel.: +49-6131-3922731, Fax: +49-6131-3924615

however, Bachant and Klymkowsky 1996). The way in which the mature 8- to 12-nm IFs are formed from tetramers is not precisely known and may involve several intermediate stages, such as “unit-length” particles, heterogeneous oligomers, and/or protofilaments (for recent reviews, see Parry and Steinert 1999; Herrmann and Aebi 2000). Given the speed and energy-independent spontaneous IF assembly *in vitro* (Herrmann and Aebi 2000), mechanisms must exist that regulate and fine-tune IF assembly *in vivo*.

CKFs are the major stabilizing elements of the epithelial cytoskeleton. Their importance for mechanical stability becomes readily apparent in heritable skin diseases in which single point mutations of CK genes are sufficient to cause severe disorders that are associated with pronounced cell fragility and reduced tissue coherence, most prominently in locations and situations of increased mechanical stress (Fuchs and Weber 1994; McLean and Lane 1995). Further evidence for the important contribution of CKF networks to epithelial resilience and the maintenance of tissue integrity has been provided in knockout and transgenic mice (Magin 1998). On the other hand, epithelial homeostasis requires that the cytoskeleton is dynamic to be able to adjust to processes such as cell division, wound healing, inflammation, intraepithelial migration, differentiation, or apoptosis of neighboring cells. Two basic molecular mechanisms have been proposed to facilitate and to contribute to CKF dynamics in these situations: association with specific polypeptides, the IFAPs (IF-associated polypeptides), and protein modification. IFAPs either act as factors favoring the soluble CK state, as is the case for protein 14-3-3 (Liao and Omary 1996) and heat-shock protein 70 (Liao et al. 1995a), or function as agents stabilizing the filamentous CK state. The latter category may include those polypeptides that facilitate the association of CKFs with each other to form thick bundles (e.g., filaggrin), with other filaments (e.g., plectin), or with the plasma membrane (e.g., desmosomal proteins, KAP85; recently reviewed in Wiche 1998; Fuchs and Yang 1999; Kowalczyk et al. 1999; Coulombe et al. 2000; Herrmann and Aebi 2000). Among polypeptide modifications that regulate CKF dynamics, phosphorylation is certainly the most important type (reviewed in Omary et al. 1998). CK phosphorylation has been shown to prevent filament formation *in vitro* (Yano et al. 1991). Accordingly, increased CK phosphorylation correlates *in vivo* with elevated levels of soluble CKs, as occurs during mitosis and meiosis (Klymkowsky et al. 1991; Chou et al. 1993; Liao et al. 1997b). Furthermore, pharmacologic interference with the balance of phosphorylation and dephosphorylation has provided striking evidence for the essential contribution of this modification to CKF network dynamics *in vivo* (Tölle et al. 1987; Cadrin et al. 1992; Deery 1993; Kasahara et al. 1993; Yatsunami et al. 1993; Baricault et al. 1994; Blankson et al. 1995; Toivola et al. 1997, 1998; Yuan et al. 1998; Feng et al. 1999; Paramio 1999; Negron and Eckert 2000). It has been demonstrated that both interaction with IFAPs and protein modifica-

tion cooperate in the regulation of CK dynamics such that CK phosphorylation affects IFAP binding (e.g., Liao et al. 1995a; Liao and Omary 1996; Ku et al. 1998; Ku and Omary 2000).

Given that CKs are dynamic structures, the way in which these intrinsically apolar filaments are altered *in vivo* is poorly understood, and the cues that regulate their organization as extended networks are unknown. The injection of CK mRNAs or labeled CK polypeptides has shown that CKF renewal and subunit exchange occurs throughout the CKF network (e.g., Miller et al. 1991, 1993; Franke et al. 1984). On the other hand, recent time-lapse fluorescence microscopy of the CKF network at steady state has indicated the importance of the cell cortex for this process (Windoffer and Leube 1999, 2001). Even more puzzling are the questions of how and where the “endless” filaments are formed to establish the complex three-dimensional IF network. Do other cytoskeletal filaments induce CKF network formation (Knapp et al. 1983; Celis et al. 1984)? Do desmosomes initiate this process (Bologna et al. 1986)? Does the nucleus act as a CKF organizing center (Eckert et al. 1982)? Does the cell cortex provide a means for regulating network dynamics (Windoffer and Leube 1999, 2001), or do other organizing centers exist in certain cellular subdomains (Knapp et al. 1983; Eckert and Caputi 1985)? Virtually nothing is known about the molecular mechanisms of the reverse process, namely the disruption of the CKF network. In a unifying working model, we have proposed that CKF network assembly and disassembly are principally reverse processes that follow similar steps and are both controlled from the cell cortex (Windoffer and Leube 2001).

To examine the principles and mechanisms of CKF network dynamics *in vivo*, we have recently established an epithelial cell line expressing fluorescently labeled CKFs (Windoffer and Leube 1999). To this end, vulva carcinoma-derived A-431 cells have been stably transfected with a cDNA construct coding for CK chimera HK13-EGFP consisting of human CK13 and the enhanced green fluorescent protein (EGFP). In A-431 clone AK13-1, we have shown that chimeras are incorporated into a normal-appearing IF cytoskeleton, which, in these cells, contains only class I and class II IF polypeptides. We have used these cells in the current study to examine the effect of the serine and threonine phosphatase inhibitor okadaic acid (OA) on the *in vivo* dynamics of the CKF network. The tumor promoter OA has been chosen since it is known to induce hyperphosphorylation of CKs and to lead to CKF network reorganization (Kasahara et al. 1993; Yatsunami et al. 1993; Chou and Omary 1994; Blankson et al. 1995). With these tools, we have observed, for the first time, the subsequent stages of CKF network breakdown *in vivo* in single interphase cells and show that they follow a specific temporospatially defined pattern, viz., an energy-dependent process that results in the formation of cytoplasmic granular aggregates before any alterations in other cytoskeletal networks are visible. These findings have implications for

the more detailed understanding of CKF dynamics and the principles governing CK reorganization during mitosis and Mallory body (MB) formation in liver disease.

## Materials and methods

### Cell culture

Human vulva carcinoma A-431 cells and stably transfected A-431 subclone AK13-1-expressing fluorescent human CK 13 chimera HK13-EGFP were as previously described (Windoffer and Leube 1999, 2001). Cells were maintained in high glucose DMEM (PAA Laboratories, Cölbe, Germany) at 37°C and 5% CO<sub>2</sub>. OA (Sigma, St. Louis, MO) was added at concentrations ranging from 0.025 µg/ml to 0.1 µg/ml for various periods of time.

### Immunofluorescence microscopy

Trypsinized cells were seeded at low density onto 12-mm glass slides. When cultures reached near confluency, cells were fixed with methanol (precooled to -20°C) for 5 min and treated with acetone (-20°C) for 15 s. After a brief wash in phosphate-buffered saline (PBS), cells were incubated with primary antibodies for 30 min at room temperature (primary antibodies were omitted in controls), washed with PBS for 10 min, incubated with secondary antibodies for 30 min, and washed again with PBS (10 min) and distilled water (2 min). The glass slides were mounted in elvanol, which was, in most instances, supplemented with Hoechst 33258 (Sigma) at 0.1 µg/ml for nuclear staining. Fluorescence was viewed in an epifluorescence microscope (Axiophot, Zeiss, Jena, Germany) and was recorded with a digital camera (Hamamatsu 4742-95, Hamamatsu, Herrsching, Germany).

Monoclonal antibodies reacting either with human CK 8 (K<sub>8</sub>-17.2), CK 13 (K<sub>13</sub>-1.1), CK 18 (K<sub>18</sub>-174), or desmoplakin (clones DP-2.15/2.17/2.20) were all kindly provided by Werner W. Franke (German Cancer Research Center, Heidelberg, Germany; cf. Windoffer and Leube 1999), and monoclonal antibodies against α-tubulin were from Amersham Pharmacia Biotech (Freiburg, Germany). Secondary antibodies (Cy3-conjugated goat anti-mouse IgGs) were from Rockland Laboratories (Gilbertsville, PA). In addition, Texas-red-coupled phalloidin (Molecular Probes, Eugene, OR) was used to label actin filaments. In this case, methanol/acetone-fixed cells were incubated with 5 U phalloidin/ml PBS for 30 min at room temperature.

### Time-lapse fluorescence microscopy

To view living cells, the recently described culture chamber was used (Windoffer and Leube 1999; Windoffer et al. 2000). During recording, cells were maintained at 37°C in phenol-red-free Hanks' medium (pH 7.4), containing Hanks' salt solution, 25 mM hydroxyethylpiperazine ethanesulfonic acid (HEPES), MEM non-essential amino acid solution, MEM amino acid solution, 100 U/ml penicillin, 100 µg/ml streptomycin (all from Life Technologies, Karlsruhe, Germany), 5% fetal calf serum, and 4.8 mM *N*-acetyl-L-cysteine (both from Sigma). The medium was exchanged in single steps by using a pump with regulatable flow rates. In some instances, OA was added to the medium at concentrations between 0.025 µg/ml and 0.1 µg/ml. For ATP depletion, 50 mM 2-deoxy-D-glucose and 0.05% sodium azide were added.

EGFP epifluorescence was recorded by using filterset no. 10 from Zeiss and a Hamamatsu digital camera (see above). HPD-CPx software (Hamamatsu) was used to retain the images and to control a shutter (Zeiss). The resulting image sequences were edited with Image-Pro Plus software (version 4.0; Media Cybernetics, Silver Spring, CA) and converted into movies (QuickTime 4.0), which are available at <http://www.uni-mainz.de/FB/Medizin/Anatomie/Leube/>. Photoshop software (Adobe Photoshop 5.0) was used to edit single pictures and to assemble figures.

### Electron microscopy

For electron microscopy, cells were grown to high density on 12-mm glass slides and treated with 0.1 µg/ml OA in high glucose DMEM for 140 min (37°C, 5% CO<sub>2</sub>). Cells were briefly washed in PBS (37°C) and fixed for 10 min at room temperature in 2% formaldehyde freshly dissolved in PBS. After being washed (2×5 min) in PBS, cells were permeabilized with 0.1% saponin (Sigma) in PBS for 5 min at room temperature and washed again with PBS (2×5 min). To block unspecific antibody-binding sites, cells were incubated for 15 min in 5% goat serum (Sigma) in PBS followed by a 5-min wash with PBS. Rabbit anti-GFP antibodies (MoBiTec, Göttingen, Germany) were applied for 2 h (this step was omitted in the negative control). After being washed (3×5 min) in PBS, cells were incubated with 1-nm gold-conjugated goat anti-rabbit IgG (Nanoprobes, Stony Brook, NY) overnight at 4°C and then washed (3×5 min) in PBS. A second fixation step followed in 2.5% glutaraldehyde in PBS for 15 min at room temperature and a wash in distilled water. For silver enhancement, cells were washed (2×10 min) in HEPES buffer (50 mM HEPES, 200 mM sucrose, pH 5.8) and then treated with HQ Silver (Nanoprobes) for 6 min followed by washes (2×5 min) in a solution containing 50 mM HEPES, 250 mM sodium thiosulfate (pH 7.5) and then in PBS (2×5 min). For final fixation, 0.2% osmium tetroxide was applied for 30 min at room temperature, followed by washes in distilled water (2×5 min). Cells were dehydrated in a graded ethanol series. Propylene oxide was used as the intermediate, and cells were embedded in Epon 812 and polymerized. Ultrathin sections were cut on a Reichert-Jung Ultramicrotome (Leica, Bensheim, Germany) and lightly stained with 8% uranyl acetate (in water) for 10 min. Grids were viewed and documented in an EM10 electron microscope (Zeiss).

## Results

### The IF cytoskeleton is completely destroyed within 5 h of OA treatment

To examine the effect of hyperphosphorylation on the structural integrity and maintenance of the CKF system, cultured cells were treated with OA, an inhibitor of serine and threonine phosphatases. As a suitable cell system, vulva carcinoma-derived A-431 clone E3, which is known for its abundance and diversity of CKs and lack of other cytoplasmic IF types, was selected (cf. Leube et al. 1988; Windoffer and Leube 1999). Figure 1 shows representative staining patterns on using antibodies against CKs 8, 13 and 18 before OA treatment and at various time points after addition of the drug. Comparable pictures were also obtained with antibodies detecting CKs 5 and 17 (not shown). As judged by phase-contrast microscopy, cells became more rounded during the first 2 h of treatment (not shown). At this time, the CKF network had become slightly coarser with thicker filament bundles and a larger mesh size (cf. 0 h with 2 h in Fig. 1). After 3–4 h, partial filament breakdown had occurred, and strongly fluorescent granules had formed, some of which were in association with filament-like structures (e.g., insert in Fig. 1j). At the same time, cells had further rounded, and peripheral pseudopodial-like extensions were noted in phase contrast micrographs (not shown). At later time points (5 h in Fig. 1), most CKFs had disappeared. Instead, an increased diffuse cytoplasmic fluorescence was seen with variable amounts

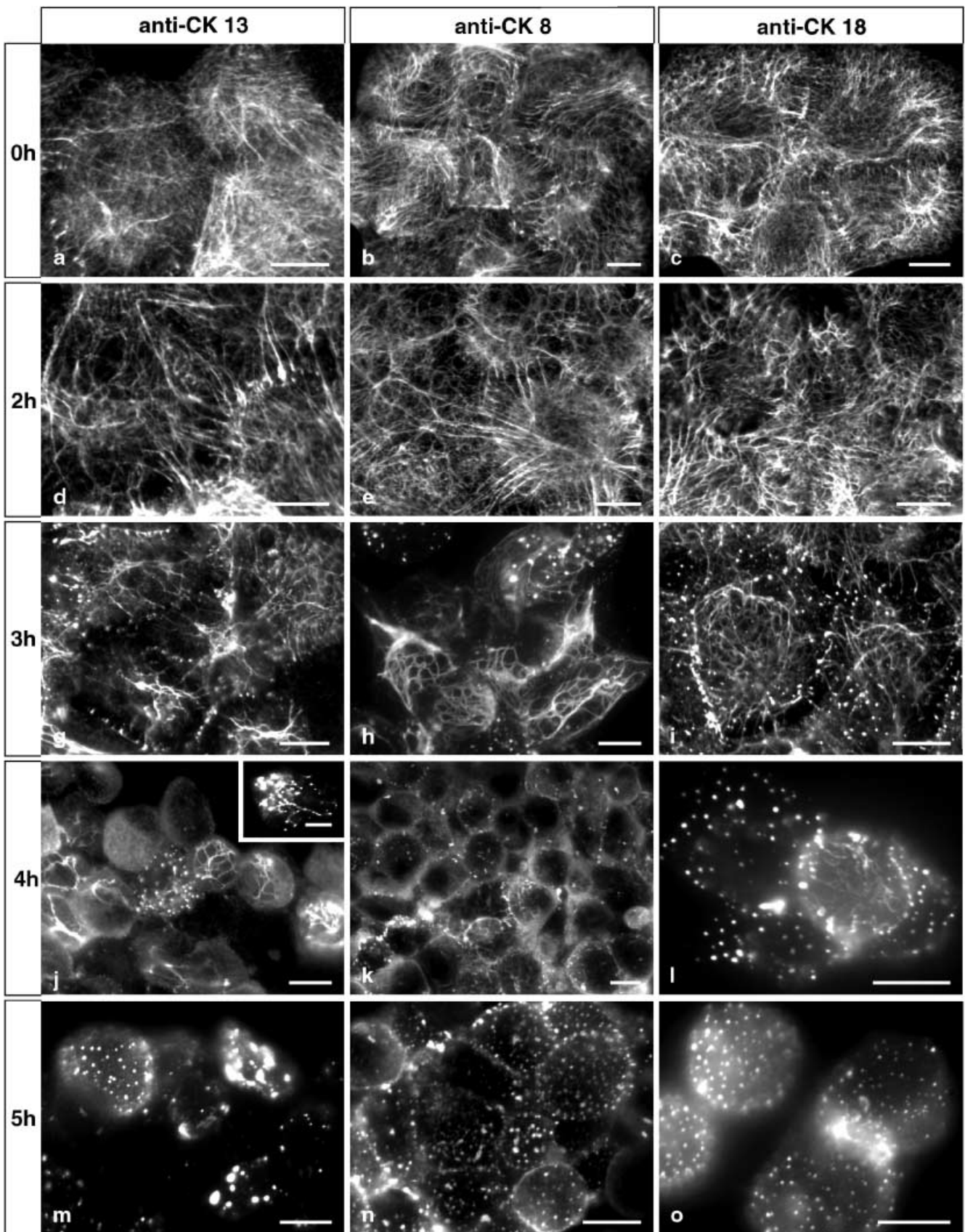


**Fig. 1a–o** Indirect immunofluorescence microscopy of methanol/acetone-fixed vulva carcinoma-derived A-431 cells treated with the phosphatase inhibitor OA (0.1  $\mu\text{g/ml}$ ); detection of CK 13 with antibody K<sub>s</sub>13.1 (*anti-CK 13*), CK 8 with antibody K<sub>s</sub>8–17.2 (*anti-CK 8*), and CK 18 with antibody K<sub>s</sub>18.174 (*anti-CK 18*). Note the changes in CK organization occurring during OA treat-

ment (duration indicated *left*) and resulting in complete filament network breakdown, the formation of granular structures, which are sometimes seen in close apposition to residual filament bundles (*insert in j*), and increased diffuse cytoplasmic fluorescence. Bars 10  $\mu\text{m}$

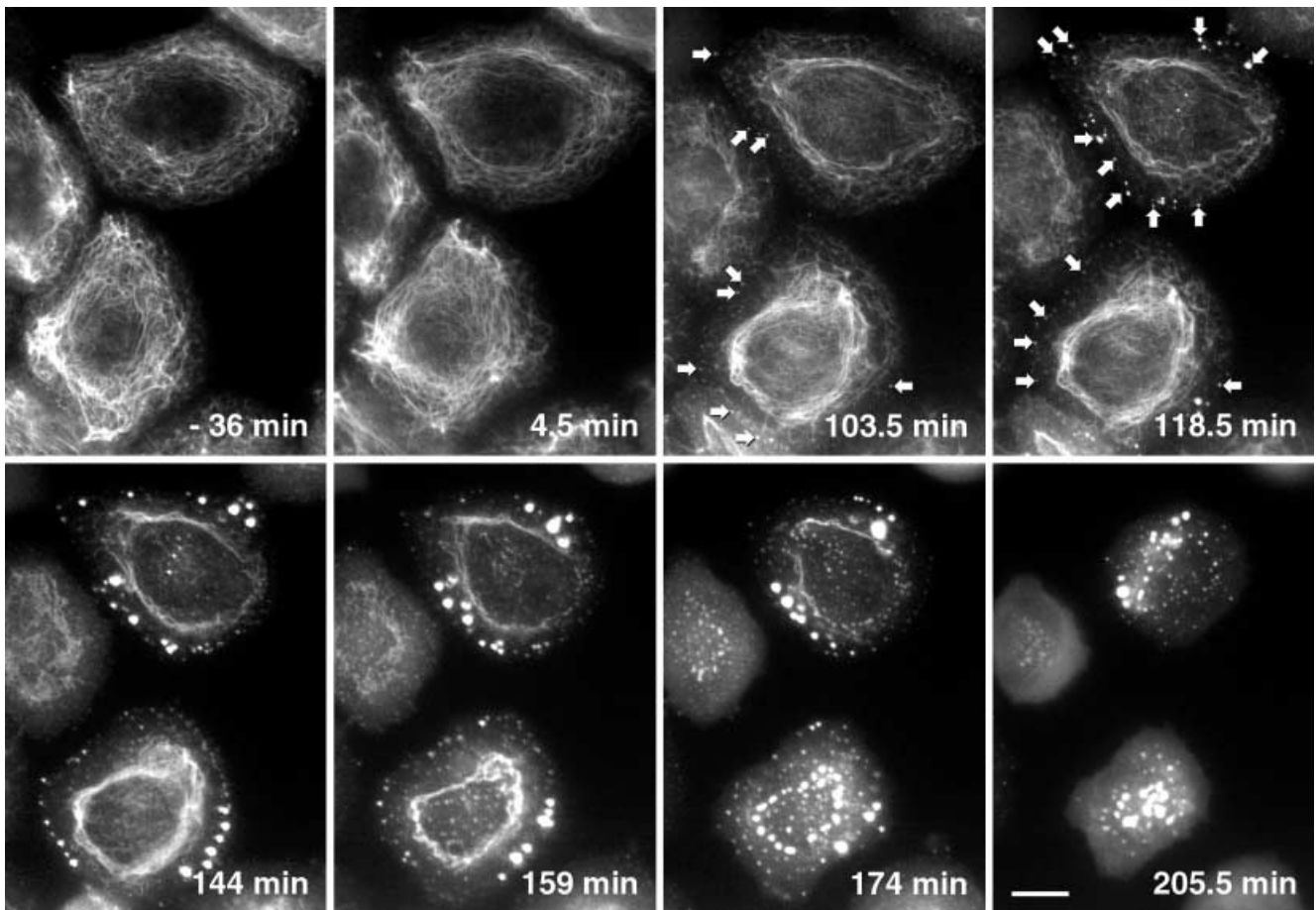


**Fig. 2** Time-lapse fluorescence microscopy of AK13-1 cells; detection of changes in the distribution of human CK 13-EGFP chimera HK13-EGFP in the presence of OA (0.025  $\mu\text{g/ml}$ ). The micrographs are taken from an image series that was recorded at 1.5-min intervals (movie 1 at <http://www.uni-mainz.de/FB/Medizin/Anatomie/Leube/>). The typical dynamics of the spread-out network prior to addition of OA are seen in the movie (-36 min to 0 min). In the presence of OA, the centripetal movement of peripheral fluorescence continues, but filaments disappear progressively starting at the periphery. Granules are formed (arrows at 103.5 min and 118.5 min) that subsequently fuse into larger aggregates (arrows in movie 1). Concurrently, a dense perinuclear ring is formed that fragments into granules toward the end of the sequence. Bar 10  $\mu\text{m}$

of spheroidal granules. The OA-induced changes affected all cells in a given culture dish similarly, but the kinetics differed somewhat between different experiments depending on the concentration of OA, temperature, and culture density. Comparable analyses were also performed in hepatocellular-carcinoma-derived PLC cells and revealed the same reaction patterns (not shown).

OA-induced cytoskeleton filament network breakdown starts at the cell periphery and proceeds centripetally

To determine whether the OA-induced CKF network disassembly occurred in distinct steps and followed a specific pattern, we used our recently established A-431

subclone AK13-1, which stably expresses fluorescent human CK 13 chimera HK13-EGFP and allows the recording of CK rearrangements in living cells by time-lapse fluorescence microscopy (Windoffer and Leube 1999). A representative experiment is documented in Fig. 2, and the accompanying movie 1 can be found at <http://www.uni-mainz.de/FB/Medizin/Anatomie/Leube/>. The characteristic interphase motility of CKFs consisting of the inwardly directed movement of diffuse and fine filamentous material in the cell periphery and of oscillations of long filaments is clearly seen in the movie before the addition of OA. These mobile properties remained the same for the next 1.5 h of OA treatment. The first signs of network disruption were then noticed in the cell periphery, and diffuse fluorescence and small granules became visible (e.g., 103.5 min in Fig. 2). Within the next 15–20 min, almost all the peripheral CKFs were lost, and additional granular aggregates appeared in this cellular subdomain (arrows at 103.5 min and 118.5 min in Fig. 2). At this time, cell morphology had hardly changed. Filament breakdown continued centripetally and was accompanied by network concentration around the nucleus. Further granules were formed, and diffuse cytoplasmic fluorescence increased. The granules were mobile, moving mostly toward the cell center and fusing to form larger structures (arrows in movie 1). During the last stages of CKF network disassembly, only a perinuclear ring of thick cables remained (159 min in Fig. 2),

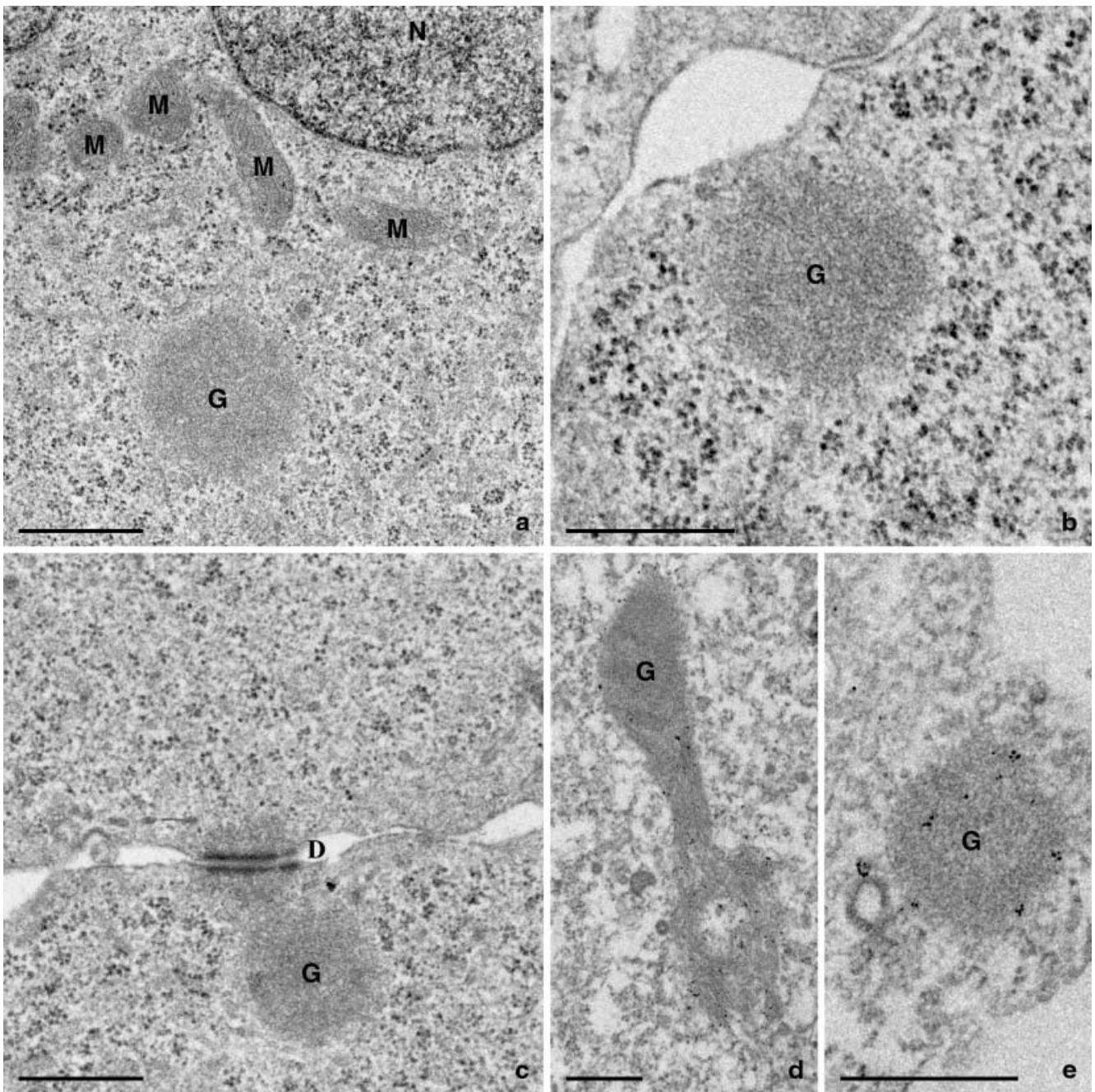


**Fig. 3a–e** Electron microscopy of HK13-EGFP-expressing AK13-1 cells that were treated with OA (0.1  $\mu\text{g/ml}$ ) for 140 min. Note the presence of spheroidal granules (*G*) and the absence of IFs and/or IF bundles. **c** A spheroid that is in the vicinity of a desmosome (*D*), which is in close association with some residual electron-dense material. **d, e** Results of immunoelectron microscopy with anti-GFP antibodies in conjunction with colloidal gold-labeled secondary antibodies and silver amplification demonstrating the detection of the HK13-EGFP in granules and their extensions. In addition, some gold particles are distributed throughout the cytoplasm with no apparent association with distinct structural elements (*N* nucleus, *M* mitochondria). Bars 500 nm

whereas the peripheral cytoplasm was completely devoid of CKFs and contained only diffuse fluorescence and granules. Finally, the perinuclear ring fragmented, producing multiple spheroids (cf. lower cell at 159 min and 174 min in Fig. 2). At the end of the sequence, all filaments had disappeared, and only multiple round bodies were detected, together with considerable diffuse fluorescence (205.5 min in Fig. 2). Pronounced cell rounding was evident at these late stages, and highly motile cytoplasmic protrusions were noticed in a few instances. The kinetics of the OA-induced changes shown in movie 1 and Fig. 2 differ somewhat from the results shown in Fig. 1, probably because of the better dispersion of OA and the stable temperature in the culture chamber used

for live-cell microscopy. Treatment of another epithelial cell line, hepatocellular-carcinoma-derived PLC cells expressing fluorescent CK 8 or CK 18 chimeras, also resulted in CKF breakdown and the formation of granules with increased diffuse cytoplasmic staining (not shown), demonstrating that the observed phenomena in AK13-1 are not restricted to a specific CK polypeptide and/or a particular cell type.

OA-induced cytokeratin accumulations are similar to mitotic spheroidal granules

Electron microscopy was performed to examine the morphology of the strongly fluorescent CK granules that were induced by OA treatment. Multiple roundish bodies with a diameter ranging between 300 nm and 1000 nm were readily identified (Fig. 3). These spheroids consisted of non-filamentous granular particles. Occasionally, aggregates were detected in the neighborhood of desmosomes (e.g., Fig. 3c). Immunoelectron microscopy confirmed that all these spheroid structures contained HK13-EGFP, although the label was mostly restricted to the peripheral parts of aggregates possibly because of epitope inaccessibility within the central regions (Fig. 3d, e). Occasionally, thick filament bundles were seen emanating from the granules (Fig. 3d). In addition, immunolabel was also detected throughout the cytoplasm. It should be noted that the morphology of the spheroids is identical to that of the previously described granular aggregates that are formed when the CKF system is transiently disrupted during mitosis (e.g., Franke et al. 1982; Lane et al. 1982).

OA-induced HK13-EGFP filament breakdown occurs without significant alterations in other cytofilaments and is precisely paralleled by the redistribution of all other cytokeratin polypeptides

The distribution of actin- and tubulin-containing filaments was examined to identify OA-induced alterations in these systems and their potential relationship to CKF network breakdown. Figure 4 shows that anti- $\alpha$ -tubulin antibodies label normal-appearing microtubules in cells, where the entire CKF network had been disassembled (cf. b and b' in Fig. 4). Similarly, the phalloidin-labeled actin filaments were still present after complete CKF disintegration, although diffuse staining had somewhat increased (Fig. 5). Thus, it is unlikely that organizational

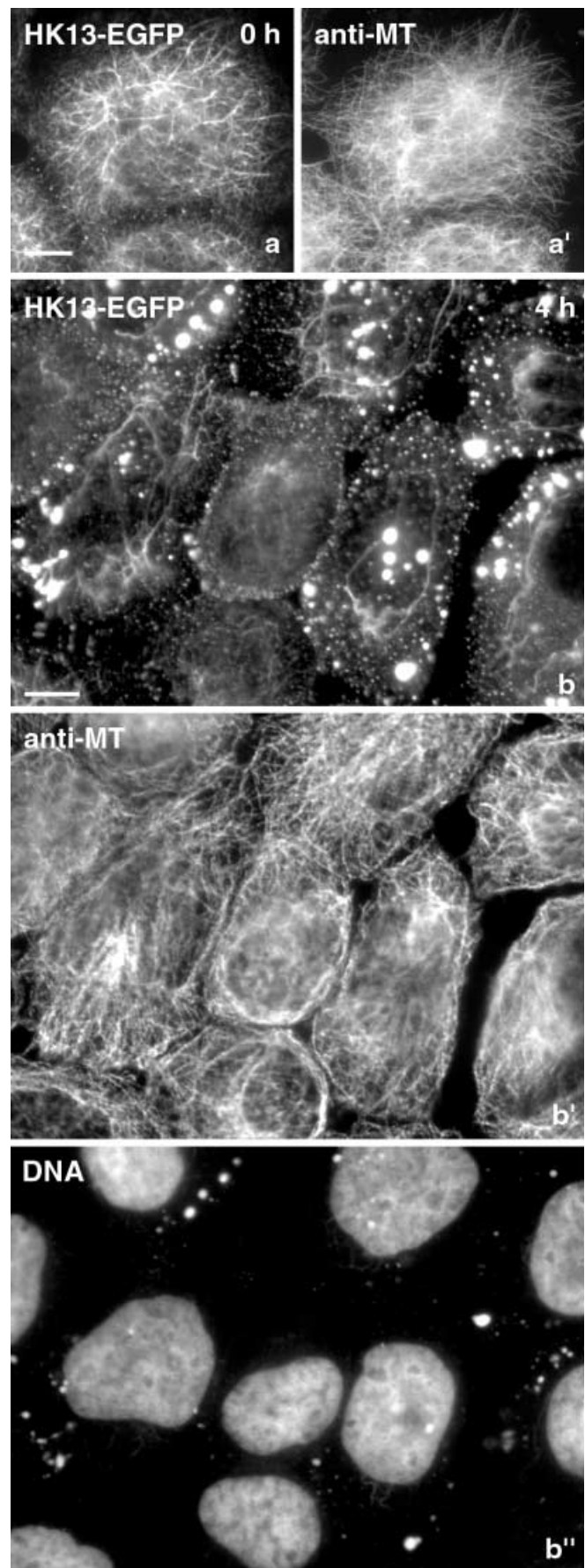


**Fig. 4** Fluorescence microscopy of methanol/acetone-fixed AK13-1 cells prior to (a, a') and after 4 h of treatment with 0.1  $\mu$ g/ml OA (b, b', b''); detection of fluorescent chimera HK13-EGFP (a, b) together with microtubules by means of anti- $\alpha$ -tubulin antibodies (a', b') and nuclei by means of Hoechst 33258 DNA stain (b''). Because of insufficient wavelength separation "bleed" through of some strongly fluorescent HK13-EGFP granules is observed in b''). Note the almost complete disassembly of the CKF network after 4 h of OA treatment, whereas microtubules and nuclei appear undisturbed. Bars 10  $\mu$ m

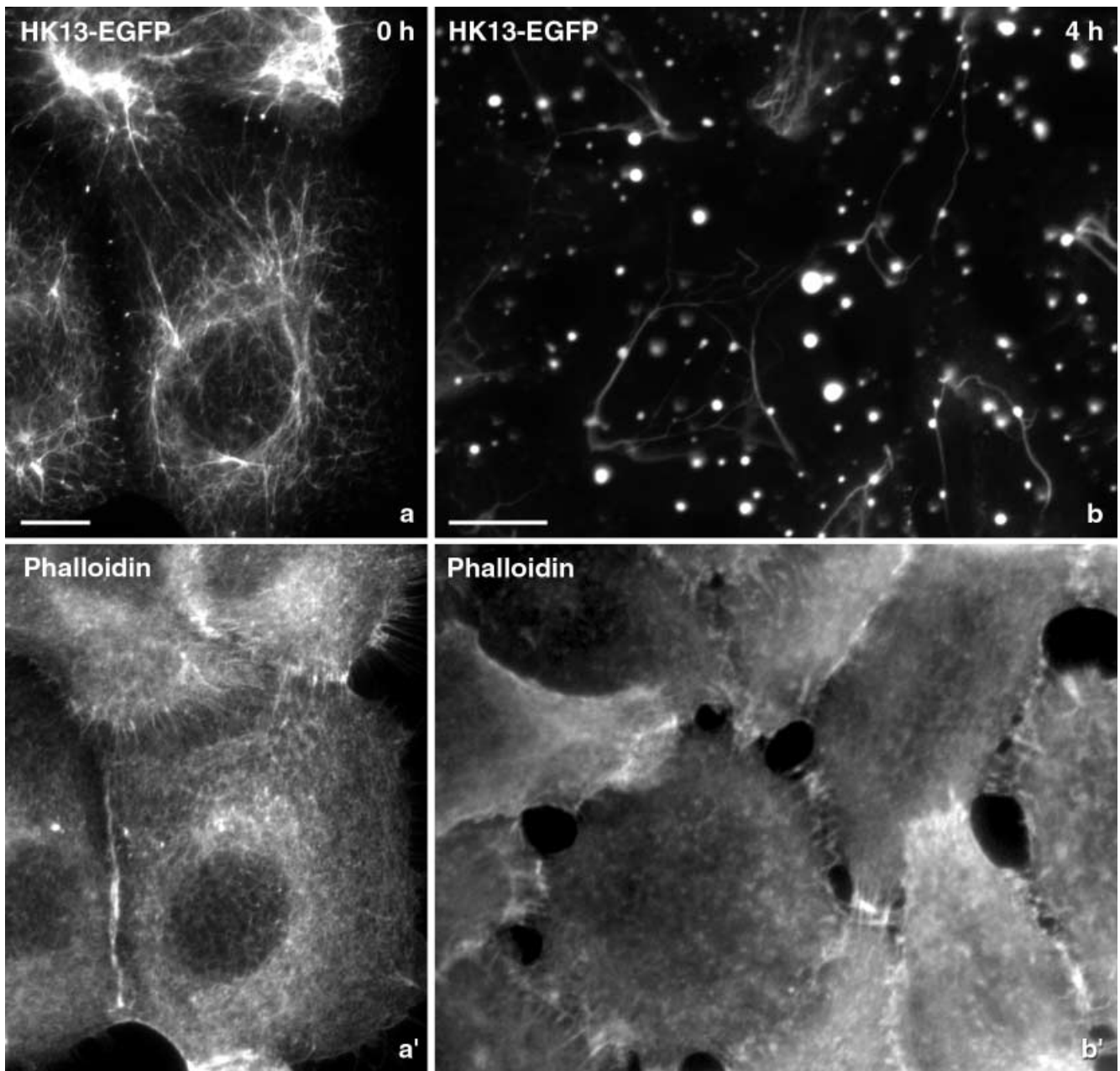


**Fig. 5** Fluorescence-microscopic analysis of methanol/acetone-fixed AK 13-1 cells before (**a, a'**) and after 4 h of treatment with 0.1  $\mu\text{g/ml}$  OA (**b, b'**). Note the complete breakdown of the CKF filament network as detected by fluorescence microscopy of chimera HK13-EGFP, whereas actin stress fibers that are labeled with Texas-red-coupled phalloidin are retained. Bars 10  $\mu\text{m}$

changes of the microtubule-based and/or actin-based systems are responsible for the OA-induced effects on HK13-EGFP-containing filaments.

The distribution of other CKs was also analyzed to determine whether OA affects the entire CKF system of AK 13-1 cells. The distribution of the fluorescent CK 13 chimera was compared by fluorescence microscopy with that of type II CK 8, a strong pairing partner of HK13-EGFP (Hofmann and Franke 1997; Fig. 6), and with that

of type I CK18, which does not directly interact on a molecular level with HK13-EGFP (Fig. 7). An almost identical fluorescence pattern was observed in each case, both in the absence of OA and during different stages of OA-induced CKF breakdown (Figs. 6, 7). Similar results were obtained with antibodies detecting other CK polypeptides, including CKs 5 and 17 (not shown).

Some OA-induced cytokeratin aggregates co-localize with desmosomal proteins

To investigate the topological relationship between CK aggregates and desmosomes, double-fluorescence microscopy was performed, comparing the distribution of the desmosomal plaque protein desmoplakin with that of

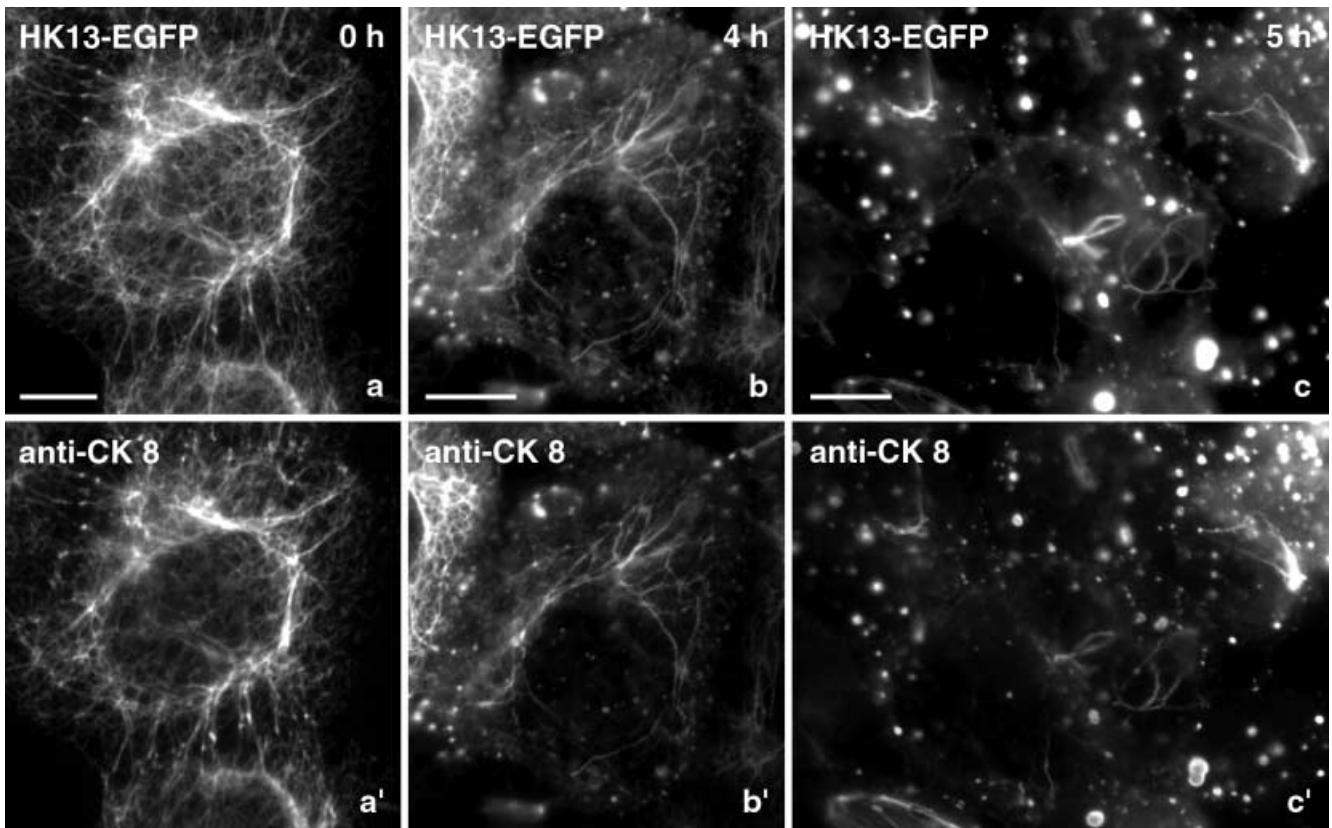


**Fig. 6** Double-fluorescence microscopy of methanol/acetone-fixed AK13-1 cells before (**a, a'**) and after a 4-h (**b, b'**) or 5-h (**c, c'**) treatment with OA (0.1  $\mu\text{g}/\text{ml}$ ); detection of chimera HK13-EGFP by epifluorescence (**a, b, c**) together with CK 8 by means of antibody K<sub>8</sub>-17.2 for indirect immunofluorescence (**a', b', c'**). Note the co-localization between structures containing HK13-EGFP together with CK 8. Bars 10  $\mu\text{m}$

HK13-EGFP during various stages of OA-induced CKF breakdown (Fig. 8). Figure 8b, b' shows that most CK granules do not co-localize with desmoplakin-positive structures (arrowheads, small arrows). On the other hand, some overlap is apparent (large arrows in Fig. 8b, b'), indicating that interactions may exist between CK granules and desmosomes. In support of this, the time-lapse fluorescence images shown in movie 1 and Fig. 2 demonstrate that granular CK aggregates are first formed in the cell periphery next to cell-cell contacts. In addition, the electron micrograph in Fig. 3c depicts a CK spheroid in close proximity to a desmosome.

No signs of apoptosis are seen in cells with completely disrupted cytokeratin filament networks

To exclude that alterations of the CKF system were caused by the induction of the proteolytic apoptotic cascade, we searched for morphological signs of apoptosis by bright-field microscopy. In most instances, the nucleus was intact with no visible alterations, and membrane blebbing was not seen prior to complete breakdown of the CKF network. Mobile cytoplasmic protrusions that

may either precede membrane blebbing or represent its first stages were only noted in cases of high concentrations of OA. Furthermore, they appeared only after all CKFs had vanished, and the cells were almost completely round. At these and even later time points, chromatin was intact with no signs of fragmentation as judged by staining with Hoechst 33258 (not shown; see also Fig. 4b'').

OA-induced cytokeratin filament network breakdown and granule formation depend on metabolic energy

The top panel of Fig. 9 and the corresponding movie 2 (<http://www.uni-mainz.de/FB/Medizin/Anatomie/Leube/>) demonstrate that the characteristic interphase motility of the CKF network in AK13-1 was rapidly and almost completely inhibited by treatment with sodium azide and deoxyglucose, suggesting that it required ATP (see also Windoffer and Leube 1999). To determine whether the OA-induced breakdown of CKF network also required metabolic energy, AK13-1 cells were first treated with OA, and sodium azide/deoxyglucose was added when the network started to disassemble. The lower panel of Fig. 9 and movie 3 (<http://www.uni-mainz.de/FB/Medizin/Anatomie/Leube/>) present fluorescence micrographs taken during such an experiment demonstrating that ATP depletion resulted in the almost instantaneous inhibition of granular aggregate mobility. In addition, no further granules were formed, and filament breakdown was slowed down considerably.

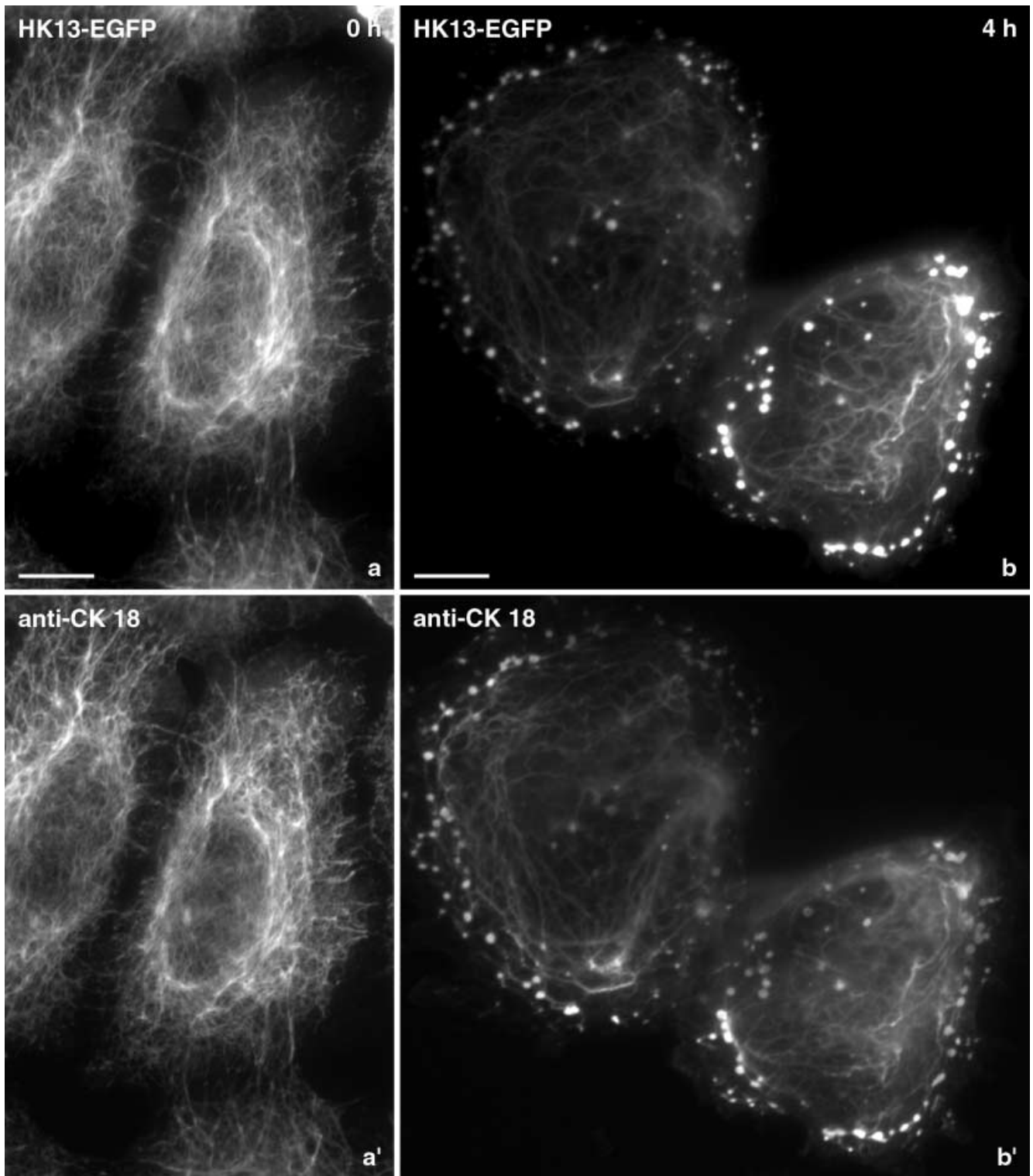


**Fig. 7** Fluorescence microscopy of methanol/acetone-fixed AK13-1 cells showing the distribution of fluorescent chimera HK13-EGFP (**a, b**) together with CK 18 by means of murine monoclonal antibody K<sub>s</sub>18.174 (**a', b'**) prior to (**a, a'**) and after (**b, b'**) 4 h of treatment with 0.1  $\mu$ g/ml OA. Note the high degree of co-localization between HK13-EGFP and CK 18 at each time point. The OA-induced alterations in **b, b'** are most prominent in the cell periphery, where many granules of different sizes are seen. Bars 10  $\mu$ m

Partial cytokeratin network disassembly and transient aggregate formation occur after a 30-min pulse of OA

To distinguish whether OA treatment initiates a self-perpetuating reaction cascade or whether its continued presence is needed for completion of CKF breakdown, AK13-1 cells were exposed to OA only briefly. Figure 10 and movie 4 (<http://www.uni-mainz.de/FB/Medi->

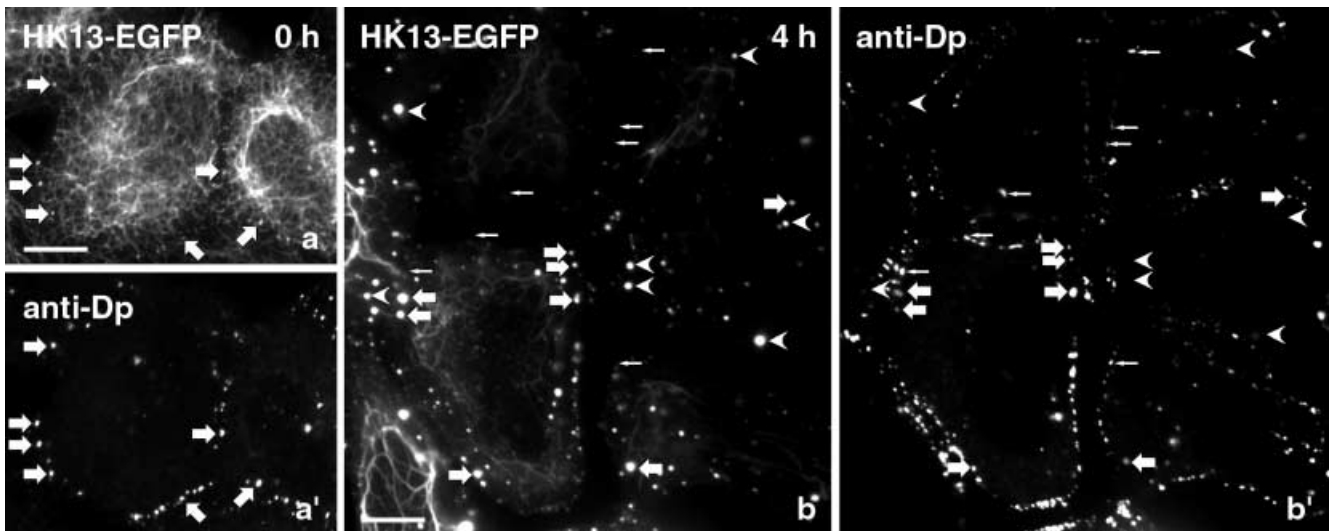


**Fig. 8** Microscopy of methanol/acetone-fixed AK13-1 cells showing the distribution of chimera HK13-EGFP as detected by epifluorescence (**a, b**) together with the desmosomal plaque protein desmoplakin, which is visualized by indirect immunofluorescence with monoclonal desmoplakin antibodies (**a', b'**) either before (**a, a'**) or after (**b, b'**) a 4-h treatment with 0.1 µg/ml OA. Note

that desmosomes remain as circumferential rings in the cell periphery (**b'**) (*large arrows* CK granules that co-localize with desmoplakin-positive structures, *arrowheads* and *small arrows* structures that contain only CK or desmoplakin, respectively). *Bars* 10 µm

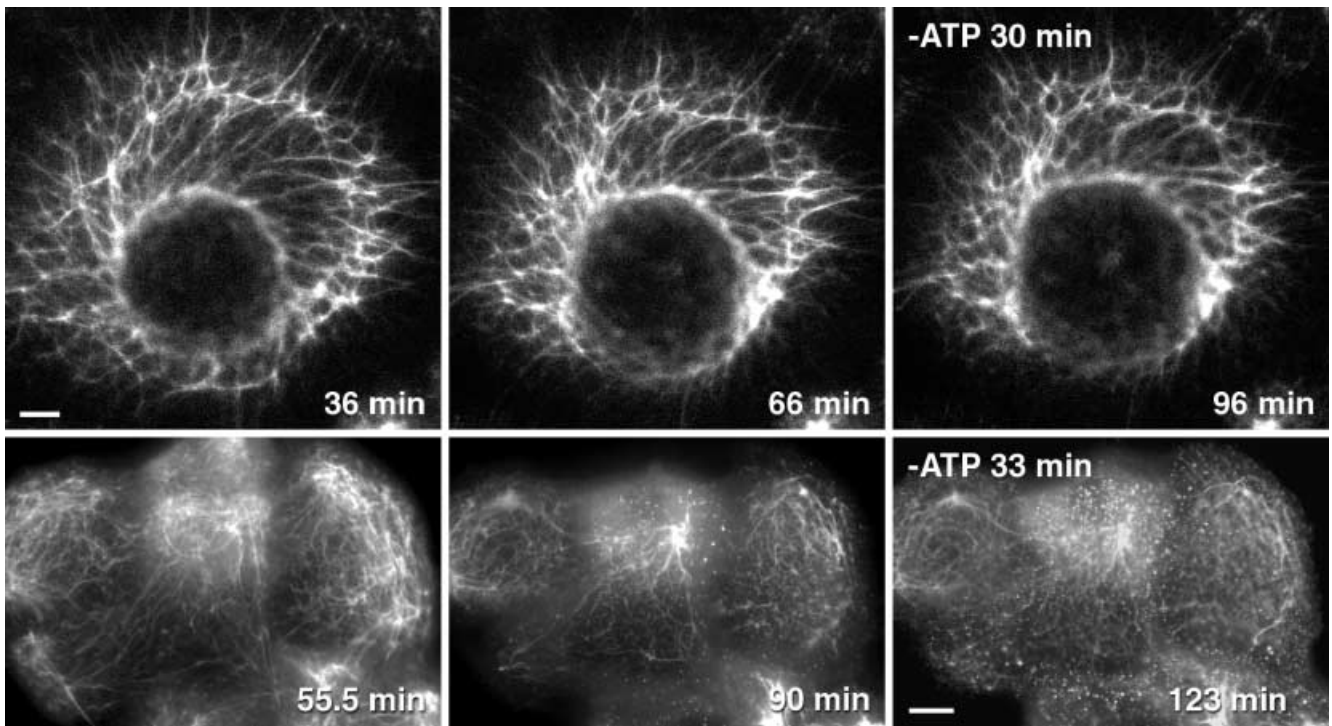


**Fig. 9** Time-lapse fluorescence microscopy of AK13-1 cells detecting altering dynamics of human CK 13-EGFP chimera HK13-EGFP in response to ATP depletion (addition of 50 mM 2-deoxy-D-glucose and 0.05% sodium azide). *Top* and movie 2 (recording at 1-min intervals; <http://www.uni-mainz.de/FB/Medizin/Anatomie/Leube/>) show first the characteristic interphase dynamics of the CKF network that is abruptly inhibited upon addition of the drugs (cf. pronounced changes between 36 min and 66 min with the lack

of significant alterations in the CKF network between 66 min and 96 min). *Bottom* and movie 3 (recording at 1.5-min intervals; <http://www.uni-mainz.de/FB/Medizin/Anatomie/Leube/>) first depict the onset of OA-induced (0.05 µg/ml) CKF network reorganization for 90 min; this is considerably slowed down by ATP depletion (-ATP). Note that granule motility, granule formation, and granule fusion do not proceed significantly and that residual filaments remain mostly unaltered. *Bar* 10 µm

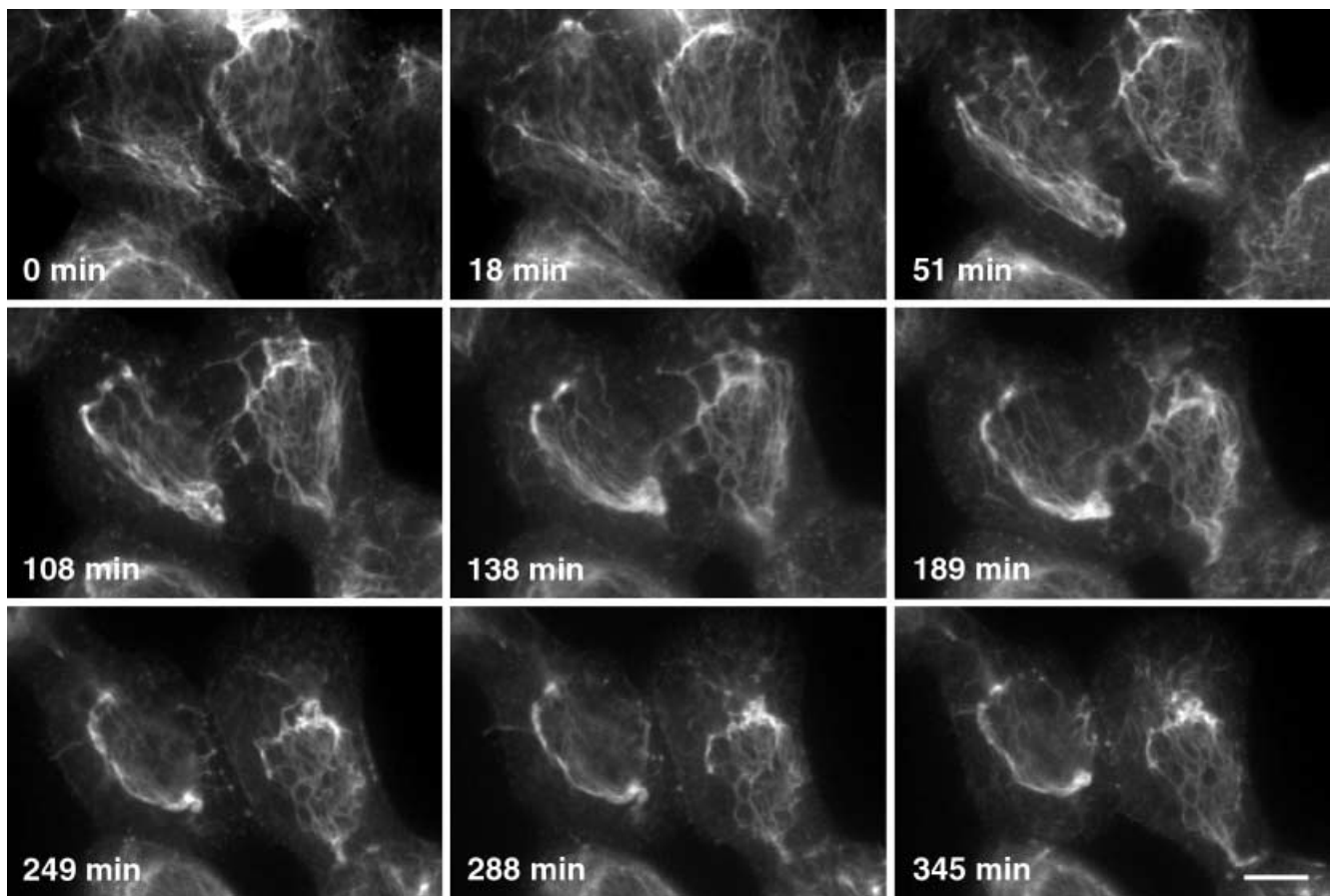


**Fig. 10** Time-lapse fluorescence microscopy of AK13-1 cells detecting HK13-EGFP during and after a short pulse of OA treatment. The micrographs are taken from movie 4 (recording at 3-min intervals; <http://www.uni-mainz.de/FB/Medizin/Anatomie/Leube/>). Cells were treated for 30 min with OA at 0.1  $\mu\text{g}/\text{ml}$  (only last 18 min of OA treatment are shown) followed by incubation in OA-free medium. A partial collapse of the CK 13 filament network after removal of the drug and the concentration of filament bundles in the perinuclear region are visible. Note, however, that the complete CKF network is not disassembled but that, instead, compacted and aggregated material remains stationary, and that no cytoplasmic aggregates are formed. In addition, a fine filamentous network is seen in the cell periphery in the last few frames. Bar 10  $\mu\text{m}$

zin/Anatomie/Leube/) show an experiment in which cells were treated with OA (0.1  $\mu\text{g}/\text{ml}$ ) for 30 min, after which time the drug was washed out and fluorescence was monitored in drug-free medium for more than 5 h. Approximately 30 min after wash-out, CKF network breakdown started in the cell periphery. However, in contrast to the sequence shown in Fig. 2, further disassembly occurred at an extremely slow pace, and the partially disrupted network was maintained throughout the rest of the observation period. Furthermore, no cytoplasmic granules were formed, and only a few, presumably desmosome-associated, accumulations were seen. Because of the absence of peripheral filaments, ongoing inward movement of cortical CK fluorescence could be clearly

resolved in the time-lapse images. Toward the end of the sequence, a very delicate and weakly fluorescent network was detectable in the cell periphery. To examine the dynamic nature of granule formation, fluorescence was also recorded in AK13-1 cells that formed granules after the 30-min pulse of OA (Fig. 11, movie 5 at <http://www.uni-mainz.de/FB/Medizin/Anatomie/Leube/>). Small granules were first seen approximately 1.5 h after removal of OA (93 min in Fig. 11) and further spheroidal aggregates were generated during the next hour (165 min in Fig. 11). Afterwards, granule formation subsided and existing granules disappeared, thus demonstrating the reversible nature of these structures. However, local aggregates and/or dense filament bundles changed only slowly and remained in the perinuclear region until the end of the recording period (321 min in Fig. 11).

## Discussion

In this study, we have induced CKF network disruption by treating cells with the polyether fatty acid and tumor promoter OA, which is the cause of diarrhetic seafood poisoning. OA is a specific inhibitor of protein phosphatases 1 and 2A and, at higher concentrations, also of phosphatase 2B (Cohen et al. 1990; Vandre and Wills 1992), thereby leading to hyperphosphorylation of CKs (Kasahara et al. 1993; Yatsunami et al. 1993; Chou and

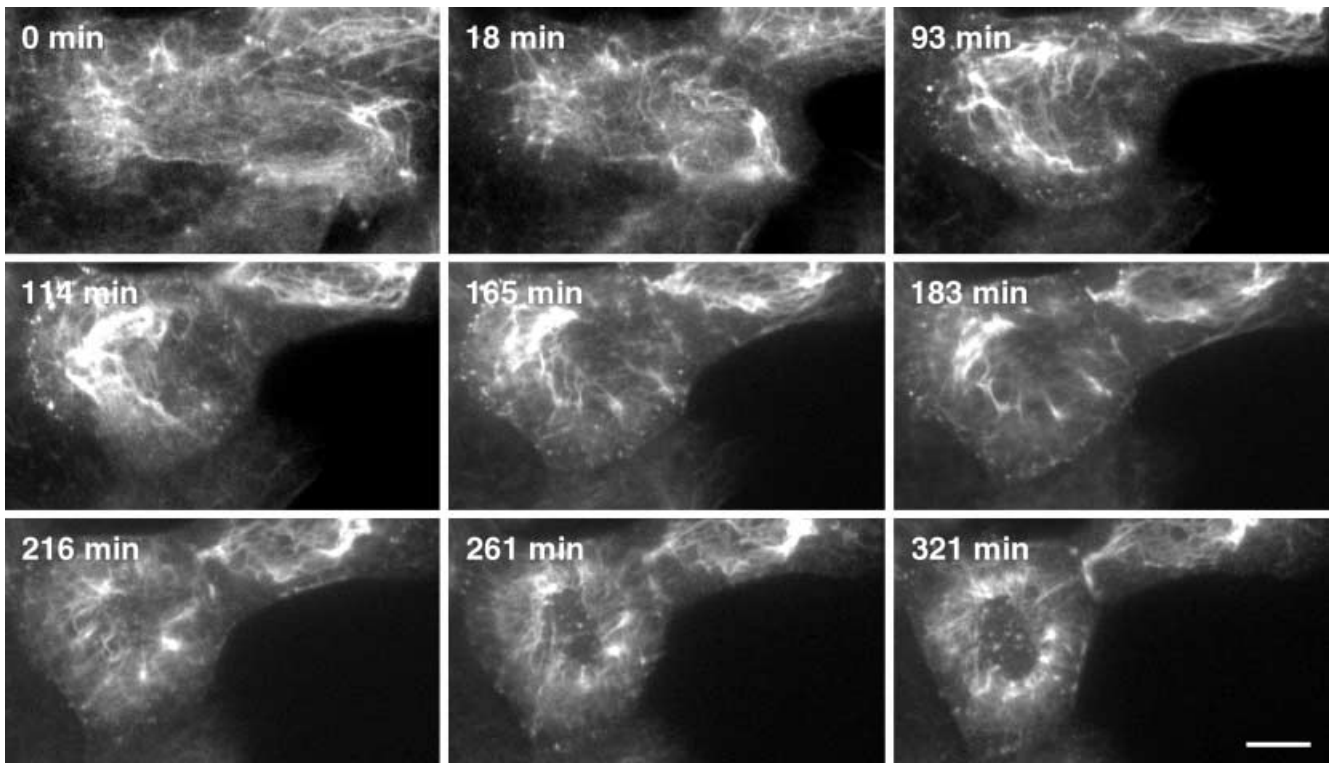


**Fig. 11** Fluorescence microscopy of living AK13-1 cells detecting HK13-EGFP during and after a short pulse of OA treatment. The micrographs are taken from movie 5 (recording at 3-min intervals; <http://www.uni-mainz.de/FB/Medizin/Anatomie/Leube/>). Cells were treated with OA (0.1  $\mu\text{g}/\text{ml}$ ; 30 min), which was removed just prior to imaging. Note the transient formation of granules in the cell periphery. Bar 10  $\mu\text{m}$

Omary 1994; Yuan et al. 1998; Paramio 1999). We have shown that this modification results in the disruption of the CKF network and the formation of granular aggregates (see also Kasahara et al. 1993; Blankson et al. 1995). Similar changes have also been noted in experiments in which alternative phosphatase inhibitors with similar properties have been used, e.g., calyculin A (Deery 1993) and *Microcystis* toxins (Falconer and Yeung 1992; Ohta et al. 1992; Toivola et al. 1997, 1998). Conversely, the activation of kinases also induces CK reorganization (Tölle et al. 1987; Cadrin et al. 1992; Paramio 1999), although the alterations are much more heterogeneous and less pronounced, often leading only to the redistribution of the CKF network (Deery 1993; Baricault et al. 1994).

OA has been shown not only to affect the organization of other IFs, albeit with different kinetics and different results (Eriksson et al. 1992; Lee et al. 1992; Sacher et al. 1992; Shea et al. 1993; Fiorentini et al. 1996; Cheng et al. 2000), but also to alter the organization of actin filaments and microtubules (Gliksman et al. 1992; Gurland and Gundersen 1993; Fiorentini et al. 1996). In the current study, however, OA has been used in vimentin-free AK13-1 cells only in concentrations that lead to the selective disassembly of the CKF network, although

we cannot exclude minor alterations in the organization and the dynamics of actin-based and tubulin-based cytoskeletal systems. The ongoing, inwardly directed movement of fluorescent material is another indication of the preservation of microtubule-dependent dynamics in OA-treated cells (Windoffer and Leube 1999). It also remains a possibility that OA-induced effects on the CKF network are not primarily attributable to modifications of CKs themselves but to alterations in CK-associated proteins such as glucose-regulated protein grp78 (Liao et al. 1997a) whose synthesis is induced in OA-treated cells through the p38 mitogen-activated protein kinase signaling pathway (Hou et al. 1993; K.-C. Chen et al. 1998; K.-D. Chen et al. 2000).

Two different mechanisms may account for the observed CKF network disassembly: either the alteration of filaments leads to their fragmentation and increased solubilization with subsequent aggregation, and/or soluble CKs are prevented from integrating into CKFs, forming instead granular aggregates. Fragmentation of the compacted perinuclear filament bundles within a short period of time during late stages of CKF network disassembly provides evidence for the first mechanism in OA-treated cells. The granular aggregates that are generated in this instance are directly derived from filamentous precursors. We have recently demonstrated that CKF fragmentation is a major mechanism responsible for the rapid CKF network disassembly observed at the onset of mitosis in AK13-1 cells (Windoffer and Leube 1999, 2001). Furthermore, the increased cytoplasmic fluorescence can be taken as an indication of an elevated soluble CK pool, which is also similar to the situation in mitotic cells with disassembling CKF networks (Windoffer and Leube

2001). We consider, however, that the main mode of OA action is via the second mechanism. Since individual CKFs have a comparatively long *in vivo* half-life (Yoon et al. 2001), it would take several hours before CKFs networks disappear, if only the integration of new subunits is inhibited. This may explain why CKF network disassembly is much slower in OA-treated cells than in mitotic cells (Windoffer and Leube 1999) and why residual filaments remain stable for several hours after OA addition. In support of this, it is generally believed that CK phosphorylation prevents filament formation (Yano et al. 1991; Inagaki et al. 1996), and available evidence indicates that phosphorylation affects preferentially the soluble CK pool (Klymkowsky et al. 1991; Kasahara et al. 1993; Liao et al. 1995c; Liao and Omary 1996; Toivola et al. 1998; Paramio 1999; see, however, Chou et al. 1993). In addition, our observation that the majority of granular aggregates is formed in the filament-free peripheral cytoplasm is another (although indirect) indication of the OA-induced inhibition of filament formation from the soluble CK pool.

Irrespective of the precise action of OA, we have been able to monitor, for the first time, the process of selective OA-induced CKF network breakdown in living epithelial cells and thus have revealed a hitherto unknown and reproducible sequence of events. Remarkably, CKF network breakdown always starts in the cell periphery. This implies that either the peripheral CKFs differ intrinsically from those present in the more central cytoplasm, making them more susceptible to OA, and/or that specific properties of the cortical compartment differentially regulate network maintenance and formation. In support of this, we have shown that diffuse CK material appears to be continuously incorporated into the peripheral IF network, thereby producing a centripetal age gradient (Windoffer and Leube 1999; Yoon et al. 2001). One can hypothesize that CKFs undergo specific maturation steps along this gradient. These could involve protein modifications or an increase in filament-packaging density, thereby affecting sensitivity to OA-induced disruption. Evidence for such CK heterogeneity has been reported by Liao et al. (1995b) and Stumtner et al. (2000), who have demonstrated the predominant localization of phosphorylated CKs in the cell periphery. In addition, desmosomal proteins and keratin-associated protein KAP85 are present at or near to the plasma membrane (Chou et al. 1994; Kowalczyk et al. 1999). Observations from our laboratory with regard to the same cells have provided evidence that the cell cortex is also an important determinant for CKF network organization during mitosis (Windoffer and Leube 2001). Biologically, regulation of CKF network formation from the cell cortex would be ideal for the epithelial cell type to be able to convey signals between the tightly associated cells and thereby to fine-tune the mechanically resistant transcellular CKF network to the specific requirements needed for epithelial plasticity. In addition, the cortical-specific regulatory mode gives direct access to the action of growth factors and other morphoregulatory molecules.

In support of this, Baribault et al. (1989) have shown that EGF-induced CKF reorganization also originates in the cell periphery.

Another distinct process that is consistently seen in the time-lapse analyses is the compaction of CKFs around the nucleus during OA treatment (cf. also Yatsunami et al. 1993; Kasahara et al. 1993). This could simply be attributable to a loss of membrane anchorage as has been observed in A-431 cells, in which desmosomes are destroyed by the expression of dominant-negative desmosomal cadherin mutants (Trojanovsky et al. 1993). It is unlikely, however, that the observed compaction is solely attributable to the release of the intrinsic tension of the CKF network since we can show that the process is slow, that it requires energy and the continued presence of OA, and that it appears to be independent of desmosomal rearrangements (see, however, Toivola et al. 1997 for contrasting results in other cells). Further contributing factors may be the OA-induced cell shape changes and the loss of long-lived detyrosinated Glu-microtubules. These have been reported to be selectively destroyed by OA treatment (Gurland and Gunderson 1993), and it has been proposed that they mediate the kinesin-dependent association of microtubules and vimentin filaments (Kreitzer et al. 1999).

The presented time-lapse analyses have also revealed hitherto unknown dynamic aspects of granular CK aggregates. They have been shown to be mobile. Interestingly, energy depletion inhibits their motility, which is reminiscent of the energy dependency of vimentin collapse (Hollenbeck et al. 1989; Tint et al. 1991). In addition, the growth and formation of granules is also disturbed by energy depletion. At this point, we cannot formally exclude that energy depletion affected the OA concentration within the cells, although the rapid effect of sodium azide and deoxyglucose treatment on one hand and the slow effect of OA wash-out on the other (Figs. 10, 11; see below) argue strongly against it. Whether the inhibition of ATP-dependent kinases is responsible for the inhibition of granule formation and network disassembly has not been investigated. In any case, two granule populations can be distinguished that must differ fundamentally in their biogenesis: one type originates in the filament-poor cell cortex from non-filamentous material, whereas the other is formed directly from filament bundles, most notably from the perinuclear compacted material. In each case, small granules then fuse to form larger aggregates. It is noteworthy that we have not been able to distinguish different spheroid populations by electron microscopy and that these homogeneous aggregates are similar to the mitotic granules described in the literature (e.g., Franke et al. 1982; Lane et al. 1982).

The established culture system should serve as a suitable model not only for understanding aspects of mitotic CK rearrangements, but also for studying mechanisms of IF aggregate formation as it occurs in disease. With respect to the epithelial CKs, particular attention has been paid to MBs, which are a prominent feature of alcohol-

or drug-induced liver damage. These structures contain large amounts of aggregated CK fragments, which, however, often retain their filamentous appearance (e.g., Franke et al. 1979). Interestingly, MB formation involves the hyperphosphorylation of CKs (Cadrin et al. 1992; Salmhofer et al. 1994; Stumptner et al. 2000). To test whether hyperphosphorylation itself is responsible for MB formation, Yuan et al. (1998) first treated mice for 5 months with the hepatotoxic drug 3–5-diethyl-carbonyl-1–4-dehydrocollidine. After a 1-month period with no drug treatment, they injected OA intraperitoneally and observed that, shortly after OA injection, aggregates of CKs 8 and 18 started to be formed in hepatocytes. Cells with fully developed MBs lacked CKFs altogether. Furthermore, the early CK aggregates stained positively with phosphothreonine antibodies. It will be interesting to determine to what degree the aggregate formation in liver disease follows similar principles to those shown in this paper (cf., e.g., Franke et al. 1979; Denk et al. 1985; Hazan et al. 1986; Zatloukal et al. 1991; this paper).

In conclusion, our cell system has revealed several new aspects of CK dynamics and their regulation through phosphorylation/dephosphorylation. Phosphorylation-induced dynamic reorganization of the CK system may be a basic mechanism for coping with various types of stress-imposed challenges on the epithelial cytoskeleton (Liao et al. 1995c, 1997b; Sanhai et al. 1999). Most importantly, this mechanism provides access for diverse surface receptor-regulated signaling pathways to affect the dynamic behavior of the CKF cytoskeleton in relation to epithelial differentiation and proliferation.

**Acknowledgements** The authors thank Ursula Wilhelm, Antje Leibold, Sabine Thomas, and Bernhard Beile for excellent technical assistance.

## References

- Bachant JB, Klymkowsky MW (1996) A nontetrameric species is the major soluble form of keratin in *Xenopus* oocytes and rabbit reticulocyte lysates. *J Cell Biol* 132:153–165
- Baribault H, Blouin R, Bourgon L, Marceau N (1989) Epidermal growth factor-induced selective phosphorylation of cultured rat hepatocyte 55-kD cytokeratin before filament reorganization and DNA synthesis. *J Cell Biol* 109:1665–1676
- Baricault L, Nechaud B, Sapin C, Codogno P, Denoulet P, Trugnan G (1994) The network organization and the phosphorylation of cytokeratins are concomitantly modified by forskolin in the enterocyte-like differentiated Caco-2 cell line. *J Cell Sci* 107:2909–2918
- Blankson H, Holen I, Seglen PO (1995) Disruption of the cytokeratin cytoskeleton and inhibition of hepatocytic autophagy by okadaic acid. *Exp Cell Res* 218:522–530
- Bologna M, Allen R, Dulbecco R (1986) Organization of cytokeratin bundles by desmosomes in rat mammary cells. *J Cell Biol* 102:560–567
- Cadrin M, McFarlane-Anderson N, Aasheim LH, Kawahara H, Franks DJ, Marceau N, French SW (1992) Differential phosphorylation of CK8 and CK18 by 12-*O*-tetradecanoyl-phorbol-13-acetate in primary cultures of mouse hepatocytes. *Cell Signal* 4:715–722
- Celis JE, Small JV, Larsen PM, Fey SJ, Mey J de, Celis A (1984) Intermediate filaments in monkey kidney TC7 cells: focal centers and interrelationship with other cytoskeletal systems. *Proc Natl Acad Sci USA* 81:1117–1121
- Chen K-C, Chen L-Y, Huang H-L, Lieu C-H, Chang Y-N, Chang MD-T, Lai Y-K (1998) Involvement of p38 mitogen-activated protein kinase signaling pathway in the rapid induction of the 78-kDa glucose-regulated protein in 9L rat brain tumor cells. *J Biol Chem* 273:749–755
- Chen K-D, Lai M-T, Cho J-H, Chen L-Y, Lai Y-K (2000) Activation of p38 mitogen-activated protein kinase and mitochondrial  $Ca^{2+}$ -mediated oxidative stress are essential for the enhanced expression of *grp78* induced by the protein phosphatase inhibitors okadaic acid and calyculin A. *J Cell Biochem* 76:585–595
- Cheng TJ, Lin YL, Chiang AS, Lai YK (2000) Association of protein phosphatase 2A with its substrate vimentin intermediate filaments in 9L rat brain tumor cells. *J Cell Biochem* 79:126–138
- Chou CF, Omary MB (1994) Mitotic arrest with anti-microtubule agents or okadaic acid is associated with increased glycoprotein terminal GlcNAcs. *J Cell Sci* 107:1833–1843
- Chou CF, Riopel CL, Rott LS, Omary MB (1993) A significant soluble keratin fraction in “simple” epithelial cells. Lack of an apparent phosphorylation and glycosylation role in keratin solubility. *J Cell Sci* 105:433–444
- Chou CF, Riopel CL, Omary MB (1994) Identification of a keratin-associated protein that localizes to a membrane compartment. *Biochem J* 298:457–463
- Cohen P, Holmes CFB, Tsukitani Y (1990) Okadaic acid: a new probe for the study of cellular regulation. *Trends Biochem Sci* 15:98–102
- Coulombe PA, Fuchs E (1990) Elucidating the early stages of keratin filament assembly. *J Cell Biol* 111:153–169
- Coulombe PA, Bousquet O, Ma L, Yamada S, Wirtz D (2000) The “ins” and “outs” of intermediate filament organization. *Trends Cell Biol* 10:420–428
- Deery WJ (1993) Role of phosphorylation in keratin and vimentin filament integrity in cultured thyroid epithelial cells. *Cell Motil Cytoskeleton* 26:325–339
- Denk H, Lackinger E, Cowin P, Franke WW (1985) Maintenance of desmosomes in mouse hepatocytes after drug-induced rearrangement of cytokeratin filament material. Demonstration of independence of desmosomes and intermediate-sized filaments. *Exp Cell Res* 161:161–171
- Eckert BS, Caputi SE (1985) Relation of the intermediate filament distribution center to keratin filament dynamics in vivo: cells at the edge of an experimental wound. *Ann N Y Acad Sci* 455:343–353
- Eckert BS, Daley RA, Parysek LM (1982) Assembly of keratin onto PtK<sub>1</sub> cytoskeletons: evidence for an intermediate filament organizing center. *J Cell Biol* 92:575–578
- Eriksson JE, Brautigan DL, Vallee R, Olmsted J, Fujiki H, Goldman RD (1992) Cytoskeletal integrity in interphase cells requires protein phosphatase activity. *Proc Natl Acad Sci USA* 89:11093–11097
- Falconer IR, Yeung DSK (1992) Cytoskeletal changes in hepatocytes induced by *Microcystis* toxins and their relation to hyperphosphorylation of cell proteins. *Chem Biol Interact* 81:181–196
- Feng L, Zhou X, Liao J, Omary MB (1999) Pervanadate-mediated tyrosine phosphorylation of keratins 8 and 19 via a p38 mitogen-activated protein kinase-dependent pathway. *J Cell Sci* 112:2081–2090
- Fiorentini C, Matarrese P, Fattorossi A, Donelli G (1996) Okadaic acid induces changes in the organization of F-actin in intestinal cells. *Toxicol* 34:937–945
- Franke WW, Denk H, Schmid E, Osborn M, Weber K (1979) Ultrastructural, biochemical, and immunologic characterization of Mallory bodies in livers of griseofulvin-treated mice. Fimbriated rods of filaments containing prekeratin-like polypeptides. *Lab Invest* 40:207–220
- Franke WW, Schmid E, Grund C, Geiger B (1982) Intermediate filament proteins in nonfilamentous structures: transient disintegration and inclusion of subunit proteins in granular aggregates. *Cell* 30:103–113

- Franke WW, Schmid E, Mittnacht S, Grund C, Jorcano JL (1984) Integration of different keratins into the same filament system after microinjection of mRNA for epidermal keratins into kidney epithelial cells. *Cell* 36:813–825
- Fuchs E, Weber K (1994) Intermediate filaments: structure, dynamics, function, and disease. *Annu Rev Biochem* 63:345–382
- Fuchs E, Yang Y (1999) Crossroads on cytoskeletal highways. *Cell* 98:547–550
- Gliksmann NR, Parsons SF, Salmon ED (1992) Okadaic acid induces interphase to mitotic-like microtubule dynamic instability by inactivating rescue. *J Cell Biol* 119:1271–1276
- Gurland G, Gundersen GG (1993) Protein phosphatase inhibitors induce the selective breakdown of stable microtubules in fibroblasts and epithelial cells. *Proc Natl Acad Sci USA* 90:8827–8831
- Hatzfeld M, Franke WW (1985) Pair formation and promiscuity of cytokeratins: formation in vitro of heterotypic complexes and intermediate-sized filaments by homologous and heterologous recombinations of purified polypeptides. *J Cell Biol* 101:1826–1841
- Hatzfeld M, Weber K (1990) The coiled coil of in vitro assembled keratin filaments is a heterodimer of type I and II keratins: use of site-specific mutagenesis and recombinant protein expression. *J Cell Biol* 110:1199–1210
- Hazan R, Denk H, Franke WW, Lackinger E, Schiller DL (1986) Change of cytokeratin organization during development of Mallory bodies as revealed by a monoclonal antibody. *Lab Invest* 54:543–553
- Herrmann H, Aebi U (2000) Intermediate filaments and their associates: multi-talented structural elements specifying cytoarchitecture and cytodynamics. *Curr Opin Cell Biol* 12:79–90
- Hofmann I, Franke WW (1997) Heterotypic interactions and filament assembly of type I and type II cytokeratin in vitro: viscometry and determinations of relative affinities. *Eur J Cell Biol* 72:122–132
- Hollenbeck PJ, Bershadsky AD, Pletjushkina OY, Tint IS, Vasiliev JM (1989) Intermediate filament collapse is an ATP-dependent and actin-dependent process. *J Cell Sci* 92:621–631
- Hou M-C, Shen C-H, Lee W-C, Lai Y-K (1993) Okadaic acid as an inducer of the 78-kDa glucose-regulated protein in 9L rat brain tumor cells. *J Cell Biochem* 51:91–101
- Inagaki I, Matsuoka Y, Tsujimura K, Ando S, Tokui T, Takahashi T, Inagaki N (1996) Dynamic property of intermediate filaments: regulation by phosphorylation. *Bioessays* 18:481–487
- Kasahara K, Kartasova T, Ren X, Ikuta T, Chida K, Kuroki T (1993) Hyperphosphorylation of keratins by treatment with okadaic acid of BALB/MK-2 mouse keratinocytes. *J Biol Chem* 268:23531–23537
- Klymkowsky MW, Maynell LA, Nislow C (1991) Cytokeratin phosphorylation, cytokeratin filament severing and the solubilization of the maternal mRNA Vg1. *J Cell Biol* 114:787–797
- Knapp LW, O'Guin WM, Sawyer RH (1983) Drug-induced alterations of cytokeratin organization in cultured epithelial cells. *Science* 219:501–503
- Kowalczyk AP, Bornslaeger EA, Norvell SM, Palka HL, Green KJ (1999) Desmosomes: intercellular adhesive junctions specialized for attachment of intermediate filaments. *Int Rev Cytol* 185:237–302
- Kreitzer G, Liao G, Gundersen GG (1999) Detyrosination of tubulin regulates the interaction of intermediate filaments with microtubules in vivo via a kinesin-dependent mechanism. *Mol Biol Cell* 10:1105–1118
- Ku NO, Omary MB (2000) Keratins turn over by ubiquitination in a phosphorylation-modulated fashion. *J Cell Biol* 149:547–552
- Ku NO, Liao J, Omary MB (1998) Phosphorylation of human keratin 18 serine 33 regulates binding to 14–3-3 proteins. *EMBO J* 17:1892–1906
- Lane EB, Goodman SL, Trejdosiewicz LK (1982) Disruption of the keratin network during epithelial cell division. *EMBO J* 1:1365–1372
- Lee WC, Yu JS, Yang SD, Lai YK (1992) Reversible hyperphosphorylation and reorganization of vimentin intermediate filaments by okadaic acid in 9L rat brain tumor cells. *J Cell Biochem* 49:378–393
- Leube RE, Bader BL, Bosch FX, Zimbelmann R, Achtstaetter T, Franke WW (1988) Molecular characterization and expression of the stratification-related cytokeratins 4 and 15. *J Cell Biol* 106:1249–1261
- Liao J, Omary MB (1996) 14–3-3 Proteins associate with phosphorylated simple epithelial keratins during cell cycle progression and act as a solubility cofactor. *J Cell Biol* 133:345–357
- Liao J, Lowthert LA, Ghori N, Omary MB (1995a) The 70-kDa heat shock proteins associate with glandular intermediate filaments in an ATP-dependent manner. *J Biol Chem* 270:915–922
- Liao J, Lowthert LA, Ku NO, Fernandez R, Omary MB (1995b) Dynamics of human keratin 18 phosphorylation: polarized distribution of phosphorylated keratins in simple epithelial tissues. *J Cell Biol* 131:1291–1301
- Liao J, Lowthert LA, Omary MB (1995c) Heat stress or rotavirus infection of human epithelial cells generates a distinct hyperphosphorylated form of keratin 8. *Exp Cell Res* 219:348–357
- Liao J, Ku N-O, Omary MB (1997a) Stress, apoptosis, and mitosis induce phosphorylation of human keratin 8 at Ser-73 in tissues and cultured cells. *J Biol Chem* 272:17565–17573
- Liao J, Price D, Omary MB (1997b) Association of glucose-regulated protein (grp78) with human keratin 8. *FEBS Lett* 417:316–320
- Magin TM (1998) Lessons from keratin transgenic and knockout mice. *Subcell Biochem* 31:141–172
- McLean WH, Lane EB (1995) Intermediate filaments in disease. *Curr Opin Cell Biol* 7:118–125
- Miller RK, Vikstrom K, Goldman RD (1991) Keratin incorporation into intermediate filament networks is a rapid process. *J Cell Biol* 113:843–855
- Miller RK, Khuon S, Goldman RD (1993) Dynamics of keratin assembly: exogenous type I keratin rapidly associates with type II keratin in vivo. *J Cell Biol* 122:123–135
- Moll R (1998) Cytokeratins as markers of differentiation in the diagnosis of epithelial tumors. *Subcell Biochem* 31:205–262
- Negron G, Eckert BS (2000) Role of phosphorylation in ethanol-induced aggregation of keratin intermediate filaments. *Alcohol Clin Exp Res* 24:1343–1352
- Ohta T, Nishiwaki R, Yatsunami J, Komori A, Suganuma M, Fujiki H (1992) Hyperphosphorylation of cytokeratins 8 and 18 by microcystin-LR, a new liver tumor promoter, in primary cultured rat hepatocytes. *Carcinogenesis* 13:2443–2447
- Omary MB, Ku NO, Liao J, Price D (1998) Keratin modifications and solubility properties in epithelial cells and in vitro. *Subcell Biochem* 31:105–140
- Paramio JM (1999) A role for phosphorylation in the dynamics of keratin intermediate filaments. *Eur J Cell Biol* 78:33–43
- Parry DA, Steinert PM (1999) Intermediate filaments: molecular architecture, assembly, dynamics and polymorphism. *Q Rev Biophys* 32:99–187
- Quinlan RA, Cohlberg JA, Schiller DL, Hatzfeld M, Franke WW (1984) Heterotypic tetramer (A<sub>2</sub>D<sub>2</sub>) complexes of non-epidermal keratins isolated from cytoskeletons of rat hepatocytes and hepatoma cells. *J Mol Biol* 178:365–388
- Sacher MG, Athlan ES, Mushynski WE (1992) Okadaic acid induces the rapid and reversible disruption of the neurofilament network in rat dorsal root ganglion neurons. *Biochem Biophys Res Commun* 186:524–130
- Salmhofer H, Rainer I, Zatloukal K, Denk H (1994) Posttranslational events involved in griseofulvin-induced keratin cytoskeleton alterations. *Hepatology* 20:731–740
- Sanhai WR, Eckert BS, Yeagle PL (1999) Altering the state of phosphorylation of rat liver keratin intermediate filaments by ethanol treatment in vivo changes their structure. *Biochim Biophys Acta* 1429:459–466
- Shea TB, Paskevich PA, Beermann ML (1993) The protein phosphatase inhibitor okadaic acid increases axonal neurofilaments

- and neurite caliber, and decreases axonal microtubules in NB2a/d1 cells. *J Neurosci Res* 35:507–521
- Steinert PM (1990) The two-chain coiled-coil molecule of native epidermal keratin intermediate filaments is a type I-type II heterodimer. *J Biol Chem* 265:8766–8774
- Steinert PM, Marekov LN (1993) Keratin intermediate filament structure, crosslinking studies yield quantitative information on molecular dimensions and mechanism of assembly. *J Mol Biol* 230:436–452
- Stumptner C, Omary MB, Fickert P, Denk H, Zatloukal K (2000) Hepatocyte cytokeratins are hyperphosphorylated at multiple sites in human alcoholic hepatitis and in a Mallory body mouse model. *Am J Pathol* 156:77–90
- Tint IS, Hollenbeck PJ, Verkhovsky AB, Surgucheva IG, Berschadsky AD (1991) Evidence that intermediate filament reorganization is induced by ATP-dependent contraction of the actomyosin cortex in permeabilized fibroblasts. *J Cell Sci* 98:375–384
- Toivola DM, Goldman RD, Garrod DR, Eriksson JE (1997) Protein phosphatases maintain the organisation and structural interactions of hepatic keratin intermediate filaments. *J Cell Sci* 110:23–33
- Toivola DM, Omary MB, Ku NO, Peltola O, Baribault H, Eriksson JE (1998) Protein phosphatase inhibition in normal and keratin 8/18 assembly-incompetent mouse strains supports a functional role of keratin intermediate filaments in preserving hepatocyte integrity. *Hepatology* 28:116–128
- Tölle HG, Weber K, Osborn M (1987) Keratin filament disruption in interphase and mitotic cells – how is it induced? *Eur J Cell Biol* 43:35–47
- Troyanovsky SM, Eshkind LG, Troyanovsky RB, Leube RE, Franke WW (1993) Contributions of cytoplasmic domains of desmosomal cadherins to desmosome assembly and intermediate filament anchorage. *Cell* 72:561–574
- Vandre DD, Wills VL (1992) Inhibition of mitosis by okadaic acid: possible involvement of a protein phosphatase 2A in the transition from metaphase to anaphase. *J Cell Sci* 101:79–91
- Wiche G (1998) Role of plectin in cytoskeleton organization and dynamics. *J Cell Sci* 111:2477–2486
- Windoffer R, Leube RE (1999) Detection of cytokeratin dynamics by time-lapse fluorescence microscopy in living cells. *J Cell Sci* 112:4521–4534
- Windoffer R, Leube RE (2001) De novo formation of cytokeratin filament networks originates from the cell cortex in A-431 cells. *Cell Motil Cytoskeleton* (in press)
- Windoffer R, Beile B, Leibold A, Thomas S, Wilhelm U, Leube RE (2000) Visualization of gap junction mobility in living cells. *Cell Tissue Res* 299:347–362
- Yano T, Tokui T, Nishi Y, Nishizawa K, Shibata M, Kikuchi K, Tsuiki S, Yamauchi T, Inagaki M (1991) Phosphorylation of keratin intermediate filaments by protein kinase C, by calmodulin-dependent protein kinase and by cAMP-dependent protein kinase. *Eur J Biochem* 197:281–290
- Yatsunami J, Komori A, Ohta T, Sukanuma M, Yuspa SH, Fujiki H (1993) Hyperphosphorylation of cytokeratins by okadaic acid class tumor promoters in primary human keratinocytes. *Cancer Res* 53:992–996
- Yoon KH, Yoon M, Moir RD, Khuon S, Flitney FW, Goldman RD (2001) Insights into the dynamic properties of keratin intermediate filaments in living epithelial cells. *J Cell Biol* 153:503–516
- Yuan QX, Nagao Y, Gaal K, Hu B, French SW (1998) Mechanisms of Mallory body formation induced by okadaic acid in drug-primed mice. *Exp Mol Pathol* 65:87–103
- Zatloukal K, Denk H, Spurey G, Lackinger E, Preisegger KH, Franke WW (1991) High molecular weight component of Mallory bodies detected by a monoclonal antibody. *Lab Invest* 62:427–434